Morphological and Isothermal Diffusive Probe Analyses of Low-Molecular-Weight Diblock Copolymers

Seong-Uk Hong,[†,‡] Jonathan H. Laurer,[§,∥] John M. Zielinski,[⊥] Jon Samseth,[⊗] Steven D. Smith,[○] J. Larry Duda,[*,†] and Richard J. Spontak[*,§]

Departments of Materials Science & Engineering and Chemical Engineering, Pennsylvania State University, University Park, Pennsylvania 16802, Departments of Materials Science & Engineering and Chemical Engineering, North Carolina State University, Raleigh, North Carolina 27695, Air Products & Chemicals Inc., Allentown, Pennsylvania 18195, Department of Physics, Institutt for Energiteknikk, N-2007 Kjeller, Norway, and Corporate Research Division, The Procter & Gamble Company, Cincinnati, Ohio 45239

Received October 15, 1997; Revised Manuscript Received February 4, 1998

ABSTRACT: While numerous scattering and rheological studies have investigated the disordering mechanism of low-molecular-weight poly(styrene-*b*-isoprene) (SI) diblock copolymers, relatively few efforts have addressed the real-space morphologies and transport properties of such copolymers at conditions near the order−disorder transition (ODT). In this work, the morphological features of seven compositionally symmetric (50/50 w/w S/I) copolymers ranging in molecular weight from 5000 to 20000, as well as several of their blends, are examined by transmission electron microscopy and small-angle neutron scattering. These results are used to interpret toluene gravimetric sorption data collected at various temperatures. At temperatures above the styrenic glass transition temperature, microphase-ordered copolymer melts are found to exhibit Fickian diffusion. In the case of a copolymer with an experimentally accessible ODT, anomalous sorption (as evidenced by equilibrium overshoot in gravimetric mass-uptake curves) is observed at temperatures near, but below, the ODT. Within the disordered state, Fickian diffusion is regained, indicating that the onset of anomalous diffusion is related to a solvent-induced ODT under isothermal conditions.

Introduction

Neat (unmodified) AB diblock copolymers exhibit a rich variety of periodic morphologies identical to those observed in low-molar-mass surfactant systems—bcc spheres of A(B) in a matrix of B(A), hexagonally packed cylinders of A(B) in a matrix of B(A), cubic bicontinuous channels of A and B, and alternating lamellae of A and B—if the A and B blocks are sufficiently incompatible.[1−3] These microstructural elements typically measure on the order of tens of nanometers and hold tremendous promise for emerging nanoscale applications.[4] Molecular characteristics governing morphological development in diblock copolymers include the Flory−Huggins interaction parameter (χ, which scales as reciprocal temperature), the number of statistical segments along the copolymer backbone (N), the volume-fraction composition of the copolymer (f_A) and the ratio of monomer asymmetry.[1,5,6] Compositionally symmetric copolymers (with A and B blocks of nearly identical volume fraction) generally exhibit the lamellar morphology due to comparable chain packing on each side of the interface separating A and B microdomains. Recent efforts[7] have, however, shown that this is not always the case for copolymers with nonlinear (e.g., miktoarm) molecular architectures. Experimental studies[3,8−10] of compositionally symmetric diblock copolymers have confirmed that the predicted[11−13] copolymer incompatibility (expressed in terms of χN) corresponding to the order−disorder transition (ODT) lies between 10 (10.495 in the mean-field, or $N \rightarrow \infty$, limit[11]) and 20, depending on the magnitude of fluctuations.

According to the mean-field portrayal of the ODT, copolymer molecules order into spatially correlated microdomains when $\chi N > (\chi N)_{ODT}$, but the copolymer remains completely structureless when $\chi N < (\chi N)_{ODT}$. If the ODT is traversed in the direction of decreasing χN (increasing temperature, T) for the sake of illustration, incorporation of composition fluctuations into this picture allows for gradual dissolution of correlated microstructure as the copolymer undergoes the transition from long-range order to disorder.[8,9,14] As this transition proceeds, copolymer molecules undergo a conformational change from being stretched along the lamellar normal to behaving as Gaussian coils.[8,9,15] In most reports of the ODT in neat diblock copolymer systems, this transition is commonly promoted by increasing T (and decreasing χ) at constant N. Common analytical methods employed to study the ODT include small-angle X-ray and neutron scattering (SAXS and SANS, respectively),[9,16−23] optical birefringence,[20,24] and dynamic rheology.[9,17,19,23,25,26] It immediately follows from the definition of copolymer incompatibility that, although not nearly as convenient as varying χ at constant N, the transition from order to disorder in a diblock copolymer can also be explored by varying N at constant T. Systematic variation of χN under conditions of constant N *and* T in a neat AB diblock copolymer can likewise be achieved through either an increase in hydrostatic pressure[27] or modification of intrablock monomer sequencing (so that A and B units comprise one or both blocks of the copolymer).[28]

* To whom correspondence should be addressed.
† The Pennsylvania State University.
‡ Present address: Polymer Hybrid Center, Korean Institute of Science & Technology, Seoul 130-650, Korea.
§ North Carolina State University.
∥ Present address: Department of Materials Science & Engineering, University of Pennsylvania, Philadelphia, PA 19104.
⊥ Air Products & Chemicals, Inc.
⊗ Institutt for Energiteknikk.
○ The Procter & Gamble Company.

S0024-9297(97)01516-7 CCC: $15.00
Published on Web 03/18/1998

Table 1. Characteristics of the Low-Molecular-Weight SI Diblock Copolymers Investigated Here

designation	$\bar{M}_n$[a]	w_S[b]	lower T_g[c] (°C)	upper T_g[c] (°C)	L_c[d] (nm)
SI5	4800	0.50			
SI8	8000	0.50			13.3
SI10	9600	0.50	−57	42	15.0
SI14	13600	0.50	−58	48	16.2 (16.8)
SI16	16000	0.50	−59	50	17.8
SI18	18000	0.50	−59	53	18.2
SI20	20000	0.50	−59	56	19.4 (18.9)

[a] From gel permeation chromatography (GPC). [b] Weight fraction of styrene, from proton nuclear magnetic resonance (^{1}H NMR). [c] From DSC at a heating rate of 20 °C/min. [d] Measured from TEM micrographs with an estimated ±7% uncertainty (values from small-angle scattering, ±3%, are provided in parentheses).

Another route by which to probe the ODT in ordered diblock copolymers, particularly those residing in the intermediate- or strong-segregation regimes (and possessing experimentally inaccessible ODTs), is through addition of a (non)selective solvent.[29−34] The presence of solvent in an ordered copolymer reduces the incompatibility of the system and, hence, the temperature corresponding to the ODT. In the case of a neutral solvent, some studies[29−32] have suggested that χN varies as $(1 - \phi_s)^{-1}$, whereas theoretical formalisms[35,36] predict, and recent experimental analyses[34] confirm, that $\chi N \sim (1 - \phi_s)^{-1.6}$ (here, ϕ_s denotes the solvent volume fraction). The ODT temperature of solvated diblock copolymers is typically discerned from small-angle scattering[30,31,33] and birefringence measurements.[32] Previously, we have provided evidence from isothermal diffusive probe analysis (IDPA) suggesting that a solvent-induced diblock copolymer ODT at constant T is signified by the onset of anomalous gravimetric sorption.[37] Anomalous sorption is characterized by solvent uptake in excess of that measured at long time. While the mechanism responsible for anomalous sorption, or equilibrium overshoot, is not yet fully understood, it is reasonable to suspect that, during solvent-induced isothermal disordering, the copolymer molecules undergo extensive conformational changes[9,15,17] due to dissolution of the interface separating adjacent A and B microdomains. Since neutral solvent molecules are predicted[36] to locate preferentially at the interface in ordered copolymers and since ordered block copolymers exhibit[38] higher solvent solubility than random copolymers of comparable composition, it follows that anomalous sorption appears to be related to interfacial dissolution at the ODT.

In this work, we examine the real- and reciprocal-space morphological characteristics of a series of low-molecular-weight poly(styrene-*b*-isoprene) (SI) diblock copolymers in which the molecular weight is varied so that the ODT of the copolymers is traversed. These results are subsequently employed to assist in the interpretation of isothermal gravimetric data collected from toluene sorption into several of the copolymers at a variety of elevated temperatures in the melt.

Experimental Section

Materials. Seven diblock copolymers with number-average molecular weight ($\bar{M}_n$) values ranging from 5000 to 20000 with polydispersities less than 1.06 (as discerned from GPC) were synthesized via living anionic polymerization in cyclohexane at 60 °C with *sec*-butyllithium as the initiator. These copolymers were all relatively symmetric (50/50 w/w S/I) according to ^{1}H NMR. Copolymer molecular characteristics and designations are listed in Table 1. The styrene block of the SI20 copolymer was 25% deuterated to enhance neutron scattering contrast. Reagent-grade toluene was obtained from Aldrich (Milwaukee, WI) for the IDPA and was used without further purification.

Methods. Films of the copolymers were prepared by casting 4% (w/v) toluene solutions into Teflon molds and removing the solvent slowly over the course of 3 weeks. The films were then heated at 90 °C for 4 h under vacuum to remove residual solvent, relax stresses induced by film formation, and promote microstructural refinement. For most of the copolymers, lower (isoprenic) and upper (styrenic) glass transition temperatures (T_gs) were measured by differential scanning calorimetry (DSC) with a Mettler Model No. 30 calorimeter. Each specimen was heated to 150 °C in the calorimeter, cooled at −10 °C/min to −100 °C and then analyzed at 20 °C/min from −100 to 150 °C under N_2. Values of these T_gs (from the inflection points on the DSC thermograms) are included in Table 1 and are found to be in good agreement with those of Krause and co-workers[39] for a variety of S-containing block copolymers. Specimens suitable for transmission electron microscopy (TEM) were obtained by cross-sectioning the bulk films in a Reichert-Jung Ultracut-S cryoultramicrotome maintained at −100 °C. Resultant sections, measuring ca. 100 nm thick, were immediately subjected to the vapor of a 2% OsO_4-(aq) solution for 90 min to stain the isoprene units. Micrographs were acquired with a Zeiss EM902 electron spectroscopic microscope operated at 80 kV and an energy loss (ΔE) of 50−100 eV. To discern correlation lengths from the images, two-dimensional Fourier transforms of the images were generated with the Digitalmicrograph software from Gatan Inc. (Pleasanton, CA).

Small-angle neutron scattering (SANS) was conducted on several copolymer blends at ambient temperature with neutrons from the 2 MW reactor source at the Institutt for Energiteknikk. The neutron wavelength was 0.50 nm, and the sample-to-detector distance was constant at 3.4 m. Two-dimensional scattering patterns were acquired with a ^{3}He detector and were corrected for detector response and normalized with respect to water. The patterns were collapsed into a one-dimensional format of scattering intensity vs scattering vector (q) by integrating azimuthally from 0 to 2π. Isothermal diffusive probe analysis using toluene vapor was conducted by gravimetric sorption on three of the seven copolymers investigated here. To ensure that the samples would not flow during solvent uptake, a small piece of each bulk film was placed inside a solid Al bucket. The bucket was suspended from a quartz spring in a thermally insulated gravimetric sorption chamber,[40] and the sample was degassed for a period of 24 h at the temperature of analysis prior to sorption. During each sequential run, the toluene vapor pressure within the chamber was increased incrementally, and the mass uptake of solvent in the film was monitored as a function of time at each increment.

Results and Discussion

Morphological Analysis. *Transmission Electron Microscopy.* Representative TEM micrographs of four microphase-ordered SI diblock copolymers are displayed as a function of descending copolymer molecular weight ($\bar{M}_n$) in Figure 1. The SI20 copolymer in Figure 1a clearly exhibits the lamellar morphology, in which the isoprene-rich lamellae appear electron opaque (dark) due to preferential OsO_4 staining. This morphology is expected for all the copolymers with $\chi N > (\chi N)_{ODT}$ due to their symmetric composition. It is also evident from this figure that the alternating lamellae resulting from quiescent microphase ordering are reasonably well-oriented. The lamellar morphology is retained in the SI18 copolymer (see Figure 1b), but some lamellae are misoriented with respect to the electron beam. While the relative fraction of misoriented lamellae is certainly dependent on specimen position and orientation relative

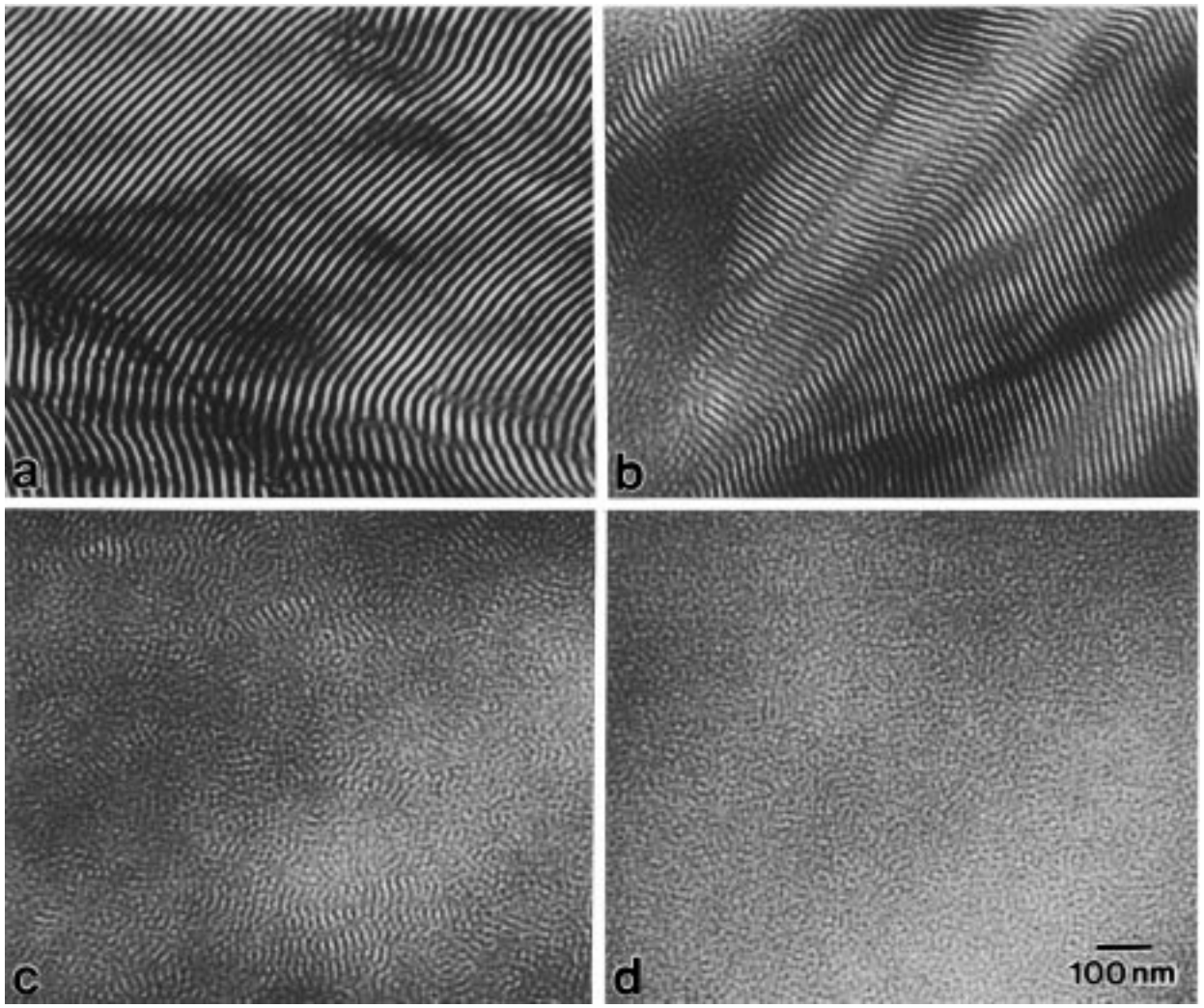

Figure 1. Series of TEM micrographs obtained from four compositionally symmetric (equimass) SI diblock copolymers that are microphase-ordered: (a) SI20, (b) SI18, (c) SI16, and (d) SI14 (sample designation and material characteristics are provided in Table 1). The isoprene-rich microdomains appear electron-opaque (dark) in these micrographs due to OsO_4 staining.

to the electron beam, this observation indicates that the lamellar grain size in the SI18 copolymer is smaller than that in the SI20 copolymer under comparable processing conditions.

As the copolymer molecular weight is decreased further, highly oriented lamellae are replaced completely by small lamellar grains measuring on the order of just a few microdomain periods in the SI16 copolymer (Figure 1c). In the case of the SI14 copolymer (Figure 1d), no indication of long-range lamellar order exists, indicating that this copolymer is relatively close to the ODT at the T_g of the styrenic block (48 °C from Table 1). Shown in Figure 2 are TEM images collected from the remaining three copolymers. Figure 2a reveals that the morphology of the SI10 copolymer, while still exhibiting two distinct T_gs (one, lower, due to the I block and one, upper, due to the S block), appears similar to that of the SI14 copolymer. According to the micrographs presented in Figure 2b and 2c, the SI8 and SI5 copolymers, respectively, do not exhibit any evidence of microphase separation and are therefore classified as microstructurally disordered, which is confirmed by the observation that these copolymers do not exhibit two T_gs (see Table 1). The structureless morphologies seen in parts b and c of Figure 2 are reminiscent of ordered block copolymers rapidly *quenched* from elevated temperatures within the disordered state.[41]

Two-dimensional Fourier transforms of the TEM micrographs in Figures 1 and 2a,b are provided in Figure 3. Comparison of these images clearly reveals that the degree of microstructural ordering, signified by the relative intensity of correlation maxima, decreases upon decreasing copolymer $\bar{M}_n$. While the intensity levels of the principal maxima in the SI20 copolymer (Figure 3a) are above the background noise threshold, the intensity of the correlation ring representative of the SI8 copolymer (Figure 3f) is comparable to the noise level, indicating negligible microdomain correlation (which is consistent with the absence of microstructure in Figure 2b). Another feature evident in these images is that the degree of lamellar orientation likewise decreases with a reduction in $\bar{M}_n$. The highly ordered microstructures of Figure 1 give rise to correlation maxima that appear as spots in Figure 3a (highly oriented lamellae lie along a single director in the SI20 copolymer) or as arcs in Figure 3b (a greater distribution of lamellar orientations exists in the SI18 copolymer). As the copolymer $\bar{M}_n$ is decreased below 18 000 (Figure 3c−f), the correlation maximum appears as an isotropic ring, which indicates no preferred microstructural orientation and which gradually fades in intensity to the background noise level upon continued reduction in $\bar{M}_n$.

Values of the average microstructural correlation length (L_c), derived from the radial positions of the

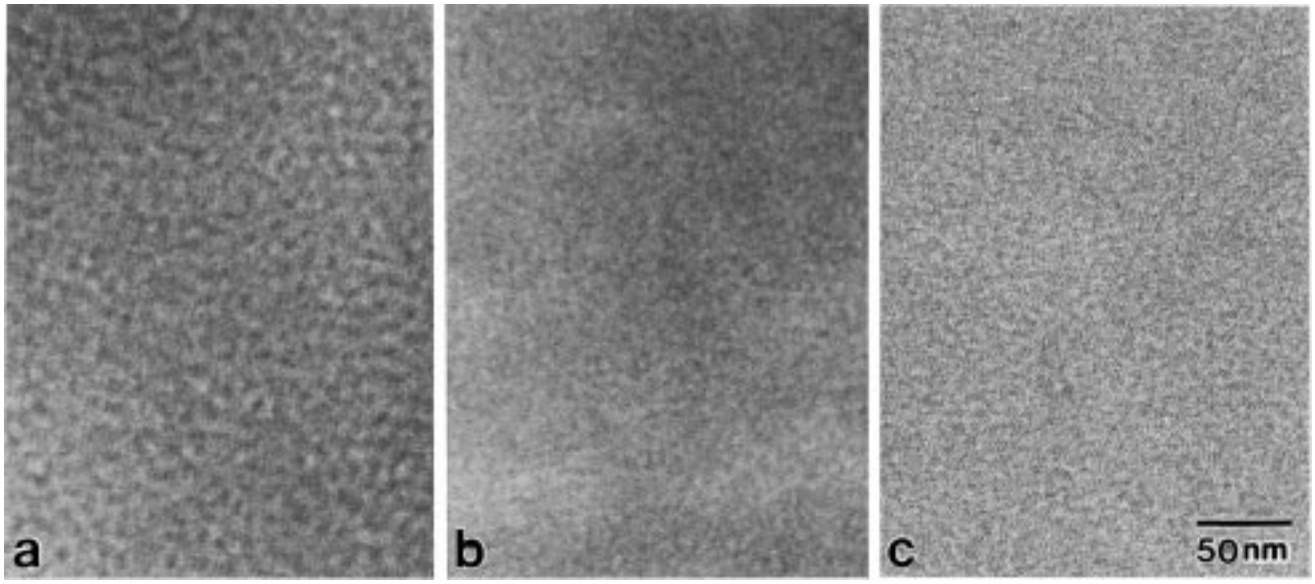

Figure 2. Three TEM micrographs of the lowest-molecular-weight copolymers investigated in this study: (a) SI10, (b) SI8, and (c) SI5. While composition fluctuations persist in micrograph (a), neither micrograph (b) nor (c) exhibits any discernible microstructure, and the copolymers corresponding to (b) and (c) are therefore presumed to be fully disordered.

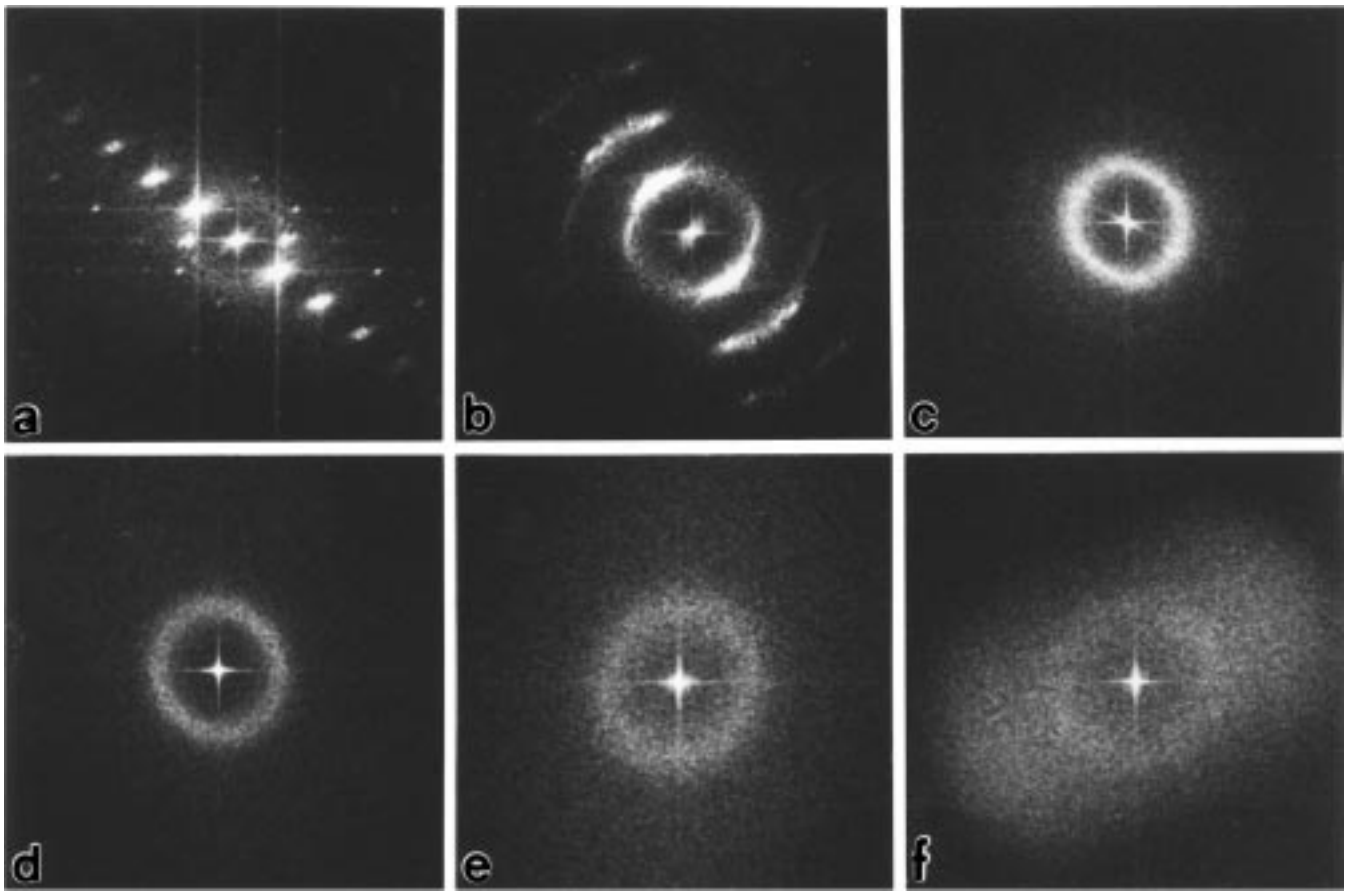

Figure 3. Two-dimensional Fourier transforms of six of the seven copolymers examined here: (a) SI20, (b) SI18, (c) SI16, (d) SI14, (e) SI10, and (f) SI8 (the transform of the SI5 copolymer image shows nothing beyond noise and is not included here for that reason). Microstructural correlation maxima appear as bright features: spots (a), arcs (b), or isotropic rings (c−f).

correlation maxima in the Fourier transforms (FTs) shown in Figure 3, are listed in Table 1 and are provided as a function of copolymer molecular weight in Figure 4. A reduction in M_n from the SI20 copolymer is accompanied by a slight, but nearly monotonic, decrease in L_c. Values of L_c obtained from the FTs in Figure 3 are seen to agree well with small-angle scattering data collected from the SI14 (SAXS[37]) and SI20 (SANS) copolymers.[42] Also shown in Figure 4 are two fitted power-law curves of the form $L_c \sim \bar{M}_n^{\alpha}$. According to Matsen and Bates,[13] α should be $\approx$0.99 for weakly segregated diblock copolymers and $\approx$0.80 for copolymers in the intermediate segregation regime. While the microscopy and scattering data in Figure 4 do not extend over a sufficiently large range in L_c or $\bar{M}_n$ to permit assessment of α, the curves are seen to describe

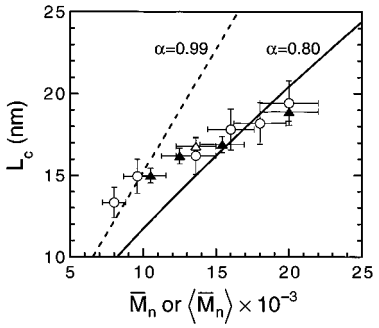

Figure 4. Microstructural correlation length (L_c) as a function of neat copolymer molecular weight, $\bar{M}_n$ (○, FT-TEM; △, SAXS[37]), or equivalent SI20/SI8 blend molecular weight, $\langle\bar{M}_n\rangle$ (▲, SANS). The solid and dashed curves correspond to power law fits of the form $L_c \sim \bar{M}_n^{\alpha}$ to the upper ($\alpha = 0.80$) and lower ($\alpha = 0.99$) ranges, respectively, of the neat copolymer data.

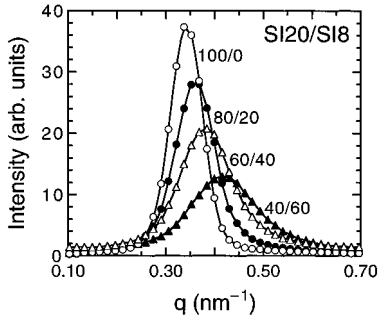

Figure 5. SANS profiles displaying integrated intensity as a function of scattering vector (q) from miscible blends of the ordered SI20 copolymer (the S block is 25% deuterated) and the disordered SI8 copolymer at four blend compositions (in w/w SI20/SI8): 100/0 (○), 80/20 (●), 60/40 (△) and 40/60 (▲). The solid lines connect the data and serve as guides for the eye.

the data within experimental uncertainty (±10% in $\bar{M}_n$, as measured by GPC).

Miscible blends of two diblock copolymers with equal compositions but different molecular weights can be envisaged[43] as neat diblock copolymers of intermediate molecular weight. If the molecular weight ratio of the two copolymers (ϵ, defined such that it is less than unity) is not far removed from unity, the characteristic correlation length varies as the average molecular weight of the blend ($\langle\bar{M}_n\rangle$) estimated from the molecular weights of the constituent copolymers.[44] In the event that ϵ differs substantially from unity, more accurate predictions for the blend correlation length are obtained from self-consistent field formalisms.[42,45,46] Shown in Figure 5 are SANS profiles obtained from several blends of the SI20 (ordered) and SI8 (disordered) copolymers, in which case $\epsilon = 0.4$. (Recall that the S block in the SI20 copolymer is 25% deuterated.) As seen in Figure 5, a correlation peak is clearly evident at a scattering vector (denoted q^*) in each profile. Corresponding values of L_c are determined from $2\pi/q^*$ (according to Bragg's law) and are listed in Table 2 and provided for comparison with values of L_c for the neat copolymers in Figure 4. Here, $\langle\bar{M}_n\rangle$ is given by $x\bar{M}_n^{(SI20)} + (1 - x)\bar{M}_n^{(SI8)}$, where x denotes the mole fraction of the SI20 copolymer in the blend. As seen in Figure 3, the correlation lengths of the SI20/SI8 blends compare favorably with those of the neat copolymers of intermediate $\bar{M}_n$. This observation is consistent with TEM and SAXS results[42,44] from SI diblock copolymer blends, as well as neutron reflectivity results[47] from mixtures of poly(styrene-*b*-methyl methacrylate) diblock copolymers.

Table 2. SANS Correlation Lengths of the SI20/SI8 Copolymer Blends

composition (w/w SI20/SI8)	x	$\langle\bar{M}_n\rangle^a$	$L_c{}^b$ (nm)
40/60	0.21	10 500	15.0
60/40	0.38	12 500	16.2
80/20	0.62	15 400	16.9
100/0	1.00	20 000	18.9

[a] Calculated from $x\bar{M}_n^{(SI20)} + (1 - x)\bar{M}_n^{(SI8)}$. [b] Measured from SANS profiles (±3%).

Isothermal Diffusive Probe Analysis. Gravimetric sorption curves have been collected from the SI14 copolymer at 25 °C, near ambient temperature (so that the S-rich lamellae are glassy), and at 50 °C, near the upper T_g of the copolymer (48 °C, according to Table 1). These results are shown in Figure 6. In this and subsequent figures, mass uptake (M_t) is presented as a function of time$^{1/2}$ and is normalized with respect to the mass uptake level at long experimental times (M_∞), which corresponds to the equilibrium solubility of the solvent in the copolymer. The shape of the curve generated from the ratio M_t/M_∞ as a function of time$^{1/2}$ (see Figure 6) provides information regarding the molecular mechanism of solvent transport into the copolymer. Diffusion is regarded as Fickian if (i) the initial part of the curve is linear with time$^{1/2}$, (ii) the curve monotonically increases to a plateau (at unity, due to the selected normalization) after long solvent-exposure times, and (iii) the curve does not exhibit an inflection point. Note that all these features are clearly evident for the curve corresponding to 25 °C in Figure 6, in which case toluene diffusion into the partially glassy SI14 copolymer appears to be Fickian near ambient temperature. With this being the case, the slope of the curve in the initial linear region yields[48] the diffusion coefficient (D) of toluene into this SI copolymer, namely, 3.55×10^{-7} cm^2/s.

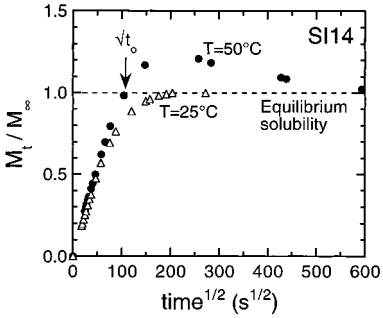

Figure 6. Isothermal diffusive probe analysis (gravimetric sorption) curves of the SI14 copolymer showing the ratio M_t/M_∞ as a function of time$^{1/2}$ at two temperatures (in °C): 25 (△) and 50 (●). The dashed line corresponds to the condition of equilibrium solvent uptake (solubility) in the copolymer, and t_o denotes the onset of equilibrium overshoot (anomalous sorption).

Similar behavior is not seen in the mass-uptake curve obtained from the SI14 copolymer at 50 °C. At a relatively short exposure time (in the frame of the experiment), the curve is observed to exceed the necessary condition that $M_t/M_\infty \rightarrow 1.0$ at long solvent exposure times. Such equilibrium overshoot, also referred to as anomalous sorption, has been observed in polymeric materials in which the chains either undergo a solvent-induced phase transition (e.g., crystallization[49]) or relax on a time scale much slower than the rate of solvent

Table 3. IDPA Data from the SI14 Diblock Copolymer at Several Temperatures

temperature (°C)	pressure (torr)		ω_s			$D \times 10^7$ (cm^2/s)	state[a] (C/S)	sorption[b]
	initial	final	initial	equilibrium	average[c]			
25	0.0	12.5	0.000	0.083	0.058	3.55	O/G	F
50	0.0	25.7	0.000	0.062[d]			O/TG	A
60	0.0	28.5	0.000	0.054	0.038	4.02	O/M	F
	28.5	61.2	0.054	0.067	0.063	5.78[e]	O/M	F
	61.2	95.4	0.067	0.122	0.106	15.9	O/M	F
	95.4	133	0.122	0.184[d]			ODT/M	A
70	0.0	28.5	0.000	0.042	0.029	4.75	O/M	F
	28.5	93.0	0.042	0.098	0.081	12.6	O/M	F
	0.0	36.8	0.000	0.053	0.037	6.03	O/M	F
	0.0	46.9	0.000	0.051	0.036	6.44	O/M	F
	46.9	92.3	0.051	0.071	0.062	9.05	O/M	F
	74.2	111	0.070	0.111[d]			ODT/M	A
	111	139	0.111	0.128[d]			ODT/M	A
80	0.0	28.5	0.000	0.027	0.019	5.16	O/M	F
	28.5	62.0	0.027	0.038[d]			ODT/M	A
	0.0	47.8	0.000	0.036[d]			ODT/M	A
	47.8	141	0.036	0.043[d]			ODT/M	A
	141	240	0.043	0.092[d]			ODT/M	A
	240	280	0.092	0.104[d]			ODT/M	A
110	0.0	59.0	0.000	0.022	0.016	12.3	D/M	F
	59.0	144	0.022	0.047	0.039	19.6	D/M	F
	144	243	0.047	0.085	0.074	29.0	D/M	F
	243	346	0.085	0.118	0.108	38.4	D/M	F
	0.0	138	0.000	0.047	0.033	18.9	D/M	F
	138	286	0.047	0.100	0.084	32.9	D/M	F
	286	404	0.100	0.158	0.141	42.0	D/M	F

[a] Copolymer (C): ordered (O), disordered (D), or neat ODT. Styrene (S): glassy (G), molten (M), or near T_g (TG). [b] Sorption is either Fickian (F) or anomalous (A). [c] Evaluated at the ω_s given by[54] ω_s(initial) + 0.7[ω_s(equilibrium) − ω_s(initial)]. [d] For anomalous sorption, this denotes the point at which the IDPA was stopped and may not represent equilibrium. [e] The mass uptake curve for this run exhibits slight curvature at early sorption times.

diffusion (due to the presence of, e.g., bulky pendant groups).[50] In the present case, the temperature at which the sorption experiment is conducted (50 °C) is very close to the upper (styrenic) T_g of the copolymer, suggesting that the anomalous sorption evident in Figure 6 is a consequence of the S-rich lamellae transforming from glassy to molten.[51] Equilibrium overshoot at 50 °C therefore constitutes a signature of the T_g transition in the SI14 copolymer. While the diffusion coefficient of toluene into the copolymer cannot be reliably extracted from mass-uptake curves exhibiting anomalous behavior, an important quantity that can be directly obtained from such curves is the time at the onset of equilibrium overshoot (denoted t_o). Measurement of t_o from curves such as the one in Figure 6 allows determination of the corresponding solvent weight fraction ($\omega_s \approx 0.060$). The experimental parameters used to generate the mass-uptake curves in this figure are listed in Table 3.

At temperatures above the T_g of the S-rich lamellae (48 °C) and below the ODT of the copolymer (83 ± 3 °C, from SAXS[37]), the copolymer is completely molten, but microphase-separated. Shown in Figure 7 are three series of sequential gravimetric sorption curves obtained from the SI14 copolymer at temperatures within the interval between T_g and the ODT: 60 (Figure 7a), 70 (Figure 7b), and 80 °C (Figure 7c). At low concentration levels of added solvent, diffusion of toluene into the copolymer at 60 °C is Fickian, confirming that the anomalous behavior observed in Figure 6 (at 50 °C) is associated[51] with the glass → melt transition of the S-rich lamellae. Once the pressure of toluene reaches 133 Torr (see Table 3) at 60 °C, a slight overshoot in M_t/M_∞ as a function of time$^{1/2}$ can be seen in Figure 7a. As in Figure 6, the onset of this overshoot in Figure 7a is denoted by t_o. Increasing the temperature of the copolymer to 70 °C (Figure 7b) results in Fickian diffusion at toluene pressures less than 93 Torr and anomalous sorption at higher pressures (up to 139 Torr). Three interesting features of the equilibrium overshoot in Figure 7b are that (i) the overshoot onset t_o appears to shift to shorter times as the toluene pressure (and fraction within the copolymer) increases, (ii) the maximum in M_t/M_∞ appears to increase with increasing pressure, and (iii) the time corresponding to the maximum in M_t/M_∞ decreases with an increase in pressure. These features, which imply that the mechanism responsible for equilibrium overshoot is more concentration dependent than the solvent diffusion, are sharply pronounced in the mass-uptake curves obtained at 80 °C (Figure 7c), since Fickian diffusion is retained at only relatively low solvent pressures (<29 Torr). In marked contrast to the IDPA results presented in Figure 7, the mass-uptake curves describing toluene sorption into the SI14 copolymer at 110 °C (above the ODT) are displayed in Figure 8 and reveal that toluene diffusion obeys Fick's law over the entire pressure range examined (up to 404 Torr) at this temperature.

The anomalous sorption behavior evident in Figure 7 cannot be ascribed to the upper (styrenic) T_g of the copolymer. Even if this T_g were relatively broad, as reported elsewhere,[39] the quantity of toluene required to induce T_g-related anomalous sorption would be expected to decrease, not increase, with increasing temperature from 50 °C, since toluene constitutes a plasticizing agent for polystyrene. This is clearly not the case in Figure 7, which shows the opposite trend, namely, anomalous sorption occurs at about 6 wt % toluene at 50 °C, but increases dramatically to 18 wt % at 60 °C. As the temperature is increased further, the toluene fraction required for anomalous sorption monotonically decreases. This concentration-temperature relationship strongly suggests that, if the equilibrium overshoot reflects a copolymer phase transition in the

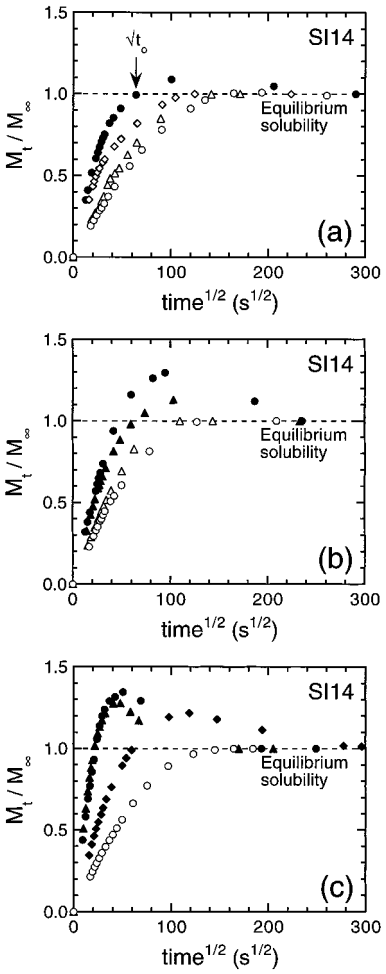

Figure 7. Mass-uptake (M_t/M_∞) curves presented as a function of time$^{1/2}$ for the SI14 copolymer at three different temperatures above the upper T_g but below the ODT of the copolymer: (a) 60 °C, (b) 70 °C, and (c) 80 °C. Toluene pressure increases as the curves shift to the left (see Table 3). Curves displaying Fickian diffusion are assigned open symbols, while those exhibiting anomalous sorption (equilibrium overshoot) are denoted by filled symbols.

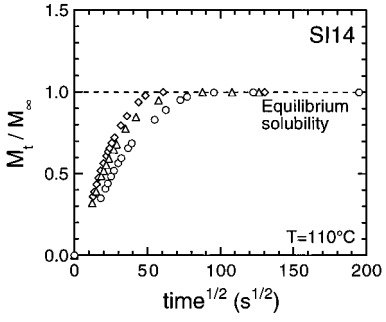

Figure 8. Gravimetric sorption curves showing M_t/M_∞ as a function of time$^{1/2}$ for the SI14 copolymer at 110 °C (which is above the copolymer ODT). In this case, all of the curves (the experimental details of which are provided in Table 3) clearly exhibit Fickian diffusion.

melt, the transition must occur at a temperature just above the highest experimental temperature examined in Figure 7 (80 °C). Since the ODT of the copolymer is 83 ± 3 °C from previous SAXS analysis,[37] it follows that the anomalous sorption seen in Figure 7 is somehow related to a solvent-induced ODT under isothermal conditions. Solvent fractions signifying the onset of equilibrium overshoot can be obtained at each temperature

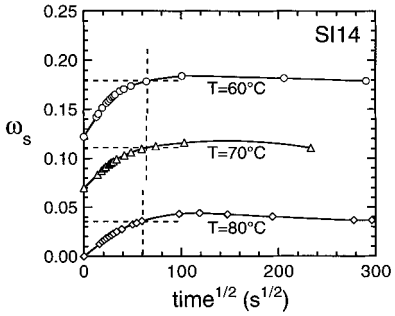

Figure 9. Dependence of solvent weight fraction (ω_s) on solvent exposure time$^{1/2}$ for the SI14 copolymer at three different temperatures (in °C): 60 (○), 70 (△), and 80 (◇). The dashed vertical lines correspond to the onset of anomalous sorption ($t_o^{1/2}$), and the dashed horizontal lines denote the value of ω_s at each of these conditions (ω_s*). The solid lines are guides for the eye.

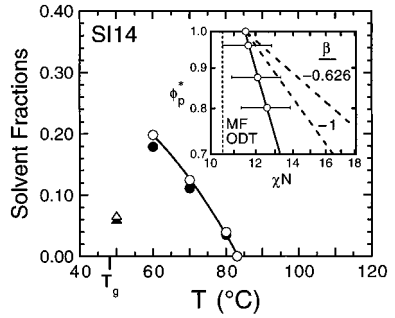

Figure 10. Variation of the solvent fractions ω_s* (filled symbols) and ϕ_s* (open symbols) with temperature for anomalous sorption observed in close proximity to the upper T_g (triangles) and ODT (circles) of the SI14 copolymer. Shown in the inset is the polymer volume fraction (ϕ_p*) as a function of χN, demonstrating that $\phi_p^* \sim (\chi N)^\beta$. The error bars reflect the ±10% uncertainty in N (due to GPC). Curves in which β is set equal to −1 and −0.626 (see ref 40) are included for comparison (dashed lines). The mean-field[11] ODT is displayed as the dotted vertical line.

from the evolution of solvent weight fraction in the copolymer (ω_s) with time$^{1/2}$ (see Figure 9). Values of ω_s extracted from Figure 9 at $t_o^{1/2}$ are designated ω_s* and are presented as a function of temperature in Figure 10. Also provided in Figure 10 are corresponding solvent volume fractions (ϕ_s*), calculated from ω_s* and the temperature-dependent mass densities of toluene,[52] as well as of the polystyrene and polyisoprene blocks comprising the copolymer.[53]

Figure 10 demonstrates that ϕ_s* decreases monotonically to 0.00 with increasing temperature. To compare these results with experimental data compiled elsewhere,[34] we present the polymer volume fraction evaluated at t_o, designated ϕ_p* (=1 − ϕ_s*), as a function of χN in the inset of Figure 10. Lodge *et al.*[34] report that χ for SI diblock copolymer melts, as well as for solvated copolymers in toluene and dioctyl phthalate, can be expressed as $33.0/T - 0.0228$. Values of χ are calculated at each IDPA temperature. From the inset, two features are immediately evident: (i) χN at the ODT of the neat SI14 copolymer (≈11.5) is slightly greater than that predicted[11] by mean-field theory, and (ii) ϕ_p* scales as $(\chi N)^\beta$, where $\beta < -1$. Also shown for comparison in the inset are predictions based on both the so-called "dilution approximation," i.e., $\phi_p^* \sim (\chi N)^{-1}$, and the theoretical treatments of Olvera de la Cruz[35] and Fredrickson and Leibler,[36] from which $\phi_p^* \sim (\chi N)^{-0.626}$. While the IDPA values of ϕ_p* obtained here exhibit a scaling

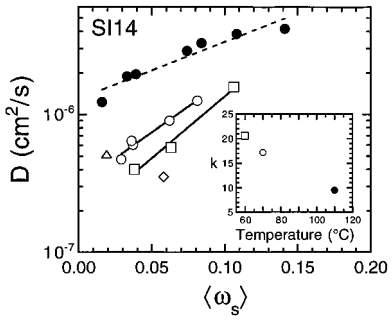

Figure 11. Diffusion coefficients (D) for toluene in the SI14 copolymer as a function of the average solvent concentration ($\langle\omega_s\rangle$) at five different temperatures (in °C): 25 (◇), 60 (□), 70 (○), 80 (△), and 110 (●). Open symbols correspond to the copolymer below its ODT. The lines reveal that ln D scales as $\langle\omega_s\rangle$, where the slope (k) is provided as a function of temperature in the inset.

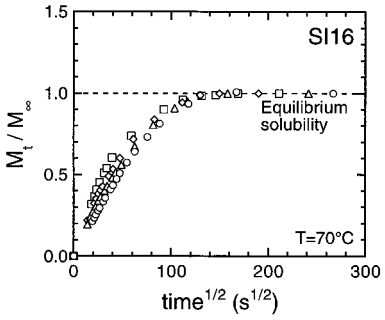

Figure 12. Mass-uptake curves presented as a function of time$^{1/2}$ for the SI16 copolymer at 70 °C for three different toluene pressure ranges. Experimental details are provided in Table 4.

relationship with respect to χN, they clearly do not obey the same dependence on χN as do solvated polymers subjected to thermal treatment. This difference may reflect the mechanism by which the copolymers undergo disordering. In conventional studies of solvated copolymers, the solvent molecules are distributed throughout the specimen as the temperature is increased. During IDPA, however, the solvent molecules must diffuse into the copolymer and try to achieve a state of local equilibrium. Solvent transport in this case is complicated considerably by copolymer fluctuations that arise during disordering. It is interesting to recognize that solvent-induced composition fluctuations within the copolymer persist at solvent compositions above ϕ_s*, as evidenced by the sorption data in Figure 7. Similarly, thermally induced fluctuations have been reported[1,8,9,17,25] for copolymers at temperatures well above the ODT.

At solvent concentrations below ϕ_s*, the sorption data provided in Figures 6−8 indicate that the diffusion of toluene into the SI14 copolymer is Fickian, in which case each data set may be analyzed to extract a diffusion coefficient (D). Corresponding values of D are included in Table 3 and are presented in Figure 11 as a function of the average solvent concentration ($\langle\omega_s\rangle$), evaluated[54] as ω_s(initial) + 0.7[ω_s(equilibrium) − ω_s(initial)]. It is evident from this figure that, under isothermal conditions, D is found to increase (by less than a factor of 4) with increasing $\langle\omega_s\rangle$ over the range of $\langle\omega_s\rangle$ examined in this work. For a given isopleth (a line of constant concentration), D likewise increases with an increase in temperature. Fitted curves included in this figure reveal that, over the solvent range examined, ln D scales linearly with $\langle\omega_s\rangle$ for the SI14 copolymer melt in both its ordered and disordered states. The extent of concentration dependence of ln D can be quantified in terms of the slope (k) of each curve.[54] Here, k, equal to $(\partial(\ln D)/\partial\langle\omega_s\rangle)_T$, is seen to decrease monotonically (almost linearly) with increasing temperature in the inset of Figure 11. Since k is the largest in magnitude for the ordered SI14 copolymer at 60 °C (in which the copolymer microphases are the most *demixed*) and decreases steadily as the temperature is increased, the observed reduction in the dependence of ln D on $\langle\omega_s\rangle$ with increasing temperature in microstructured block copolymer melts must reflect, at least in part, a corresponding increase in the extent of microphase mixing as the ODT is approached. Beyond the ODT at 110 °C, the SI14 copolymer is disordered (block mixing is complete), and k attains the lowest value of the three temperatures examined. This trend is likewise consistent with free-volume considerations,[55] from which the concentration dependence of D is expected (and typically found) to decrease with increasing temperature in polymer−solvent systems.

Most of the IDPA data collected in the present study employ the SI14 copolymer, since this copolymer possesses an ODT that is readily accessible within the gravimetric sorption chamber. In contrast, the ODT for the SI16 copolymer is expected to be significantly higher, exceeding 120 °C on the basis of the expression for χ employed earlier. To examine the sorption behavior of the ordered SI16 copolymer in the melt and to test the apparent correlation between anomalous sorption and the ODT in the solvated SI14 copolymer, IDPA has been performed on the SI16 copolymer at 70 °C. Some of the results from this analysis are shown in Figure 12. In each of the four toluene pressure (concentration) ranges investigated, Fickian diffusion is observed, further substantiating the conclusion drawn earlier[37] that anomalous sorption in the SI14 copolymer melt is a consequence of a solvent-induced ODT. Values of D derived from the isothermal sorption data in Figure 12 are listed in Table 4 and displayed as a function of $\langle\omega_s\rangle$ in Figure 13. Diffusion coefficients from the ordered SI14 copolymer melt are included in the figure for comparison. In both cases, D clearly increases with increasing $\langle\omega_s\rangle$. The curves in Figure 13 are regressed exponential fits to the data for the two copolymers and appear to possess nearly identical slopes, indicating[54] that ln D is proportional to $\langle\omega_s\rangle$ (as in Figure 11) and that the constant of proportionality is weakly dependent on $\bar{M}_n$ over the narrow molecular weight range examined.

This apparent increase in D with increasing copolymer $\bar{M}_n$ from 13 600 to 16 000 suggests, however, that penetrant diffusion increases with the extent of microphase demixing, since toluene diffuses more quickly through molten polyisoprene than through molten polystyrene at the same temperature. The degree of microphase demixing (or microphase purity) in the melt is characterized by the thermodynamic incompatibility (χN), which clearly increases with increasing $\bar{M}_n$ under isothermal conditions. Shown in Figure 14 are gravimetric sorption data from the ordered SI20 copolymer melt at 100 °C. As in the previous cases of the SI14 and SI16 copolymer melts, toluene diffusion is again found to obey Fick's law over the two pressure (concentration) ranges examined. Diffusion coefficients obtained from these data are provided in Table 4 and displayed as a function of $\langle\omega_s\rangle$ in the inset of Figure 14. Since these data have been acquired under conditions

Table 4. IDPA Data from the SI16 and SI20 Diblock Copolymers at Different Temperatures[a]

temperature (°C)	pressure (Torr) initial	pressure (Torr) final	ω_s initial	ω_s equilibrium	ω_s average	$D \times 10^7$ (cm^2/s)	state (C/S)	sorption
				SI16 Copolymer				
70	0.0	28.5	0.000	0.041	0.029	6.56	O/M	F
	28.5	73.9	0.041	0.066	0.058	11.3	O/M	F
	73.9	109	0.066	0.080	0.075	15.4	O/M	F
	109	144	0.080	0.097	0.092	20.4	O/M	F
				SI20 Copolymer				
100	0.0	38.1	0.000	0.015	0.010	5.13	O/M	F
	38.1	198	0.015	0.069	0.052	22.9	O/M	F

[a] See the footnotes in Table 3 for a description of the classifications employed here.

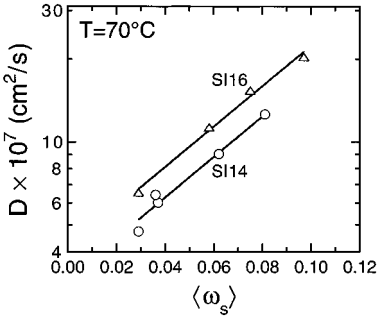

Figure 13. Diffusion coefficients of toluene in the ordered SI14 (○) and SI16 (△) copolymer melts as a function of $\langle\omega_s\rangle$ at 70 °C. The solid lines are exponential fits to the data and are seen to possess nearly identical slopes.

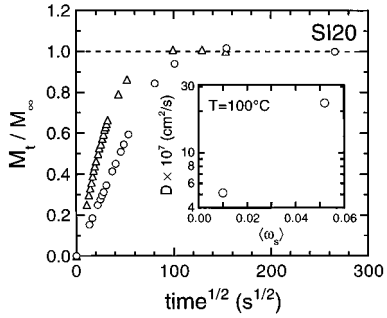

Figure 14. Variation of M_t/M_∞ with time$^{1/2}$ over two different toluene pressure (concentration) ranges for the SI20 copolymer at 100 °C. Experimental details are provided in Table 4. Diffusion coefficients extracted from the mass-uptake curves are provided as a function of $\langle\omega_s\rangle$ in the inset.

different from those employed in the investigation of the SI14 copolymer, no direct comparison can be made between the sorption behavior of the *disordered* SI14 copolymer at 110 °C and the *ordered* SI20 copolymer at 100 °C. It is interesting to note from Table 4 that the values of D obtained from the SI20 copolymer at 100 °C are greater than those from the SI16 copolymer at 70 °C despite the 30 °C increase in temperature. On the basis of the results presented in Figure 13, however, this observation suggests that χN for the SI20 copolymer at 100 °C (≈16.0 from the $\chi(T)$ correlation provided by Lodge et al.[34]) is greater than that for the SI16 copolymer at 70 °C (≈14.3).

In addition to the diffusion coefficients provided in Tables 3 and 4 and in Figures 11, 13, and 14, the solvent solubility at equilibrium constitutes another measure of solvent−copolymer interaction and can be extracted from gravimetric sorption data exhibiting Fickian behavior. [While solubility can be also discerned, in principle, from anomalous sorption data, some of these data collected at long times do not correspond to thermodynamic equilibrium due to the length of time

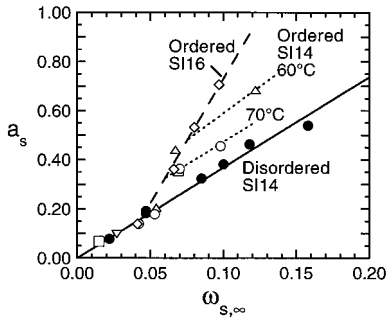

Figure 15. Solvent activity (a_s) vs equilibrium solvent fraction ($\omega_{s,\infty}$) for several SI copolymer melts at different temperatures. These include SI14 at 60 °C (△), 70 °C (○), 80 °C (▽), and 110 °C (●); SI16 at 70 °C (◇); and SI20 at 100 °C (□). The lines are linear regressions through the SI14 data (60 and 70 °C, dotted; 110 °C, solid) and the SI16 data (70 °C, dashed).

required to achieve this state.] Equilibrium solubilities are listed in Table 3 for the SI14 copolymer and in Table 4 for the SI16 and SI20 copolymers. Shown in Figure 15 is the solvent activity (a_s), defined as the ratio of the final experimental pressure to the saturated vapor pressure of toluene,[52] as a function of $\omega_{s,\infty}$, the solvent fraction at the final pressure. Several interesting features are evident in this figure. At relatively low solvent concentrations ($\omega_{s,\infty} < 0.05$), the dependence of $\omega_{s,\infty}$ on a_s for the ordered SI14 copolymer at 60, 70 and 80 °C, the ordered SI16 copolymer at 70 °C and the ordered SI20 copolymer at 100 °C is surprisingly similar to that of the disordered SI14 copolymer. For a given a_s beyond this concentration interval, however, $\omega_{s,\infty}$ is consistently the greatest in the disordered SI14 copolymer (at 110 °C).

At solvent concentrations in excess of $\omega_{s,\infty} \approx 0.05$, values of a_s for the ordered SI14, SI16, and SI20 copolymers are observed in Figure 15 to increase along a single line that represents $a_s(\omega_{s,\infty})$ for the SI16 copolymer at 70 °C. At relatively high solvent fractions, the $a_s(\omega_{s,\infty})$ line formed by connecting the data from the SI14 copolymer at 70 °C intersects that corresponding to the SI16 copolymer and exhibits a slope that is comparable to that of the disordered SI14 copolymer. A similar trend is likewise observed for the SI14 copolymer at 60 °C with two exceptions: (i) the values of a_s required to achieve the same $\omega_{s,\infty}$ at 60 °C are higher than those at 70 °C and (ii) the slope of the line connecting the SI14 copolymer data at 60 °C lies between those describing the SI14 and SI16 copolymers at 70 °C. By exclusion of the SI20 copolymer (due to insufficient data) and the SI14 copolymer at 80 °C ($\omega_{s,\infty}<0.05$), the relative incompatibilities of the SI14 and SI16 copolymers at different temperatures may be ranked as follows: SI16(70 °C) > SI14(60 °C) > SI14-(70°) > SI14(110 °C). Since the SI16 copolymer of this

series exhibits the greatest incompatibility and the most highly developed microstructure, solvent molecules are expected[36] to localize at the interfacial regions in this copolymer. As the incompatibility decreases, however, the extent of solvent localization lessens, until no localization occurs in the disordered SI14 copolymer.

This explanation of solvent activity is consistent with the anomalous sorption behavior observed in the SI14 copolymer between 60 and 80 °C. Solvent localization along the interfacial regions of the copolymer induces a reduction in copolymer incompatibility and increases as $\omega_{s,\infty}$ is increased. Upon dissolution of the interfaces as the copolymer undergoes its ODT, the solvent molecules residing at the interfaces are forced to distribute throughout the copolymer. Since, however, the solubility of solvent in the copolymer likewise decreases due to interfacial dissolution, an excess of solvent arises in the copolymer beyond the equilibrium solvent concentration. Thus, as the solvent molecules induce microstructural disordering through a reduction in copolymer incompatibility and as the solvent solubility in the copolymer simultaneously decreases, solvent molecules in excess of the equilibrium concentration are expelled from the copolymer, thereby resulting in equilibrium overshoot.

Conclusions

In this work, we have examined the morphological features and sorption properties of a series of low-molecular-weight poly(styrene-*b*-isoprene) diblock copolymers in which composition remains constant, but molecular weight is varied so that the order−disorder transition is traversed. Transmission electron micrographs reveal that the lamellar morphology characteristic of most compositionally symmetric block copolymers decreases in the extent of discernible microstructure as the copolymer molecular weight is decreased. This reduction in microstructural order is confirmed through Fourier transformation of the micrographs and small-angle neutron scattering of several blends composed of one ordered and one disordered copolymer. Isothermal diffusive probe analysis using toluene vapor has been performed on three of the ordered copolymers in the series. For one copolymer, gravimetric sorption (mass-uptake) curves are found to exhibit anomalous sorption (i.e., equilibrium overshoot) at temperatures near (i) the upper glass-transition temperature of the neat copolymer and (ii) the order−disorder transition of the copolymer melt. In the latter case, anomalous sorption becomes more pronounced and occurs at lower solvent fractions as the temperature is increased near the order−disorder transition. Since such behavior is not observed in other ordered copolymer melts at various temperatures, anomalous sorption is interpreted as a signature of a solvent-induced order−disorder transition promoted under isothermal conditions.

These results, in conjunction with solvent concentrations ascertained from mass-uptake curves exhibiting Fickian diffusion, indicate that the anomalous sorption occurs when the solvent molecules reduce the thermodynamic incompatibility of a block copolymer and cause interfacial dissolution. As both the interfacial area and solvent solubility decrease, a situation eventually arises in which the solvent molecules localized at the interfacial regions must redistribute throughout the copolymer. Since the equilibrium concentration of solvent in the copolymer is exceeded due to the reduced level of solvent solubility, solvent is expelled from the copolymer as the copolymer undergoes its order−disorder transition. While isothermal diffusive probe analysis has been previously used to investigate anomalous sorption due to solvent-induced crystallization or slow molecular relaxation, this is the first example of which we are aware that demonstrates that anomalous sorption in a block copolymer melt reflects solvent-induced microstructural disordering.

Acknowledgment. Support for this project at North Carolina State University was provided by the Shell Development Co. and, in part, by the National Science Foundation (CMS-941-2361).

References and Notes

(1) Fredrickson, G. H.; Bates, F. S. *Annu. Rev. Phys. Chem.* **1990**, *41*, 525.
(2) Förster, S.; Khandpur, A. K.; Zhao, J.; Bates, F. S.; Hamley, I. W.; Ryan, A. T.; Bras, W. *Macromolecules* **1994**, *27*, 6922.
(3) Khandpur, A. K.; Förster, S.; Bates, F. S.; Hamley, I. W.; Ryan, A. J.; Bras, W.; Almdal, K.; Mortensen, K. *Macromolecules* **1995**, *28*, 8796.
(4) Park, M.; Harrison, C.; Chaikin, P. M.; Register, R. A.; Adamson, D. H. *Science* **1997**, *276*, 1401.
(5) Hamley, I. W.; Gehlsen, M. D.; Khandpur, A. K.; Koppi, K. A.; Rosedale, J. H.; Schulz, M. F.; Bates, F. S.; Almdal, K.; Mortensen, K. *J. Phys. II* **1994**, *4*, 2161.
(6) Gehlsen, M. D.; Bates, F. S. *Macromolecules* **1994**, *27*, 3611.
(7) Tselikas, Y.; Hadjichristidis, N.; Lescanec, R. L.; Honeker, C. C.; Wohlgemuth, M.; Thomas, E. L.; *Macromolecules* **1996**, *29*, 3390.
(8) Bates, F. S.; Schulz, M. F.; Khandpur, A. K.; Förster, S.; Rosedale, J. H.; Almdal, K.; Mortensen, K. *Faraday Discuss.* **1994**, 7.
(9) Rosedale, J. H.; Bates, F. S.; Almdal, K.; Mortensen, K.; Wignall, G. D. *Macromolecules* **1995**, *28*, 1429.
(10) Karatasos, K.; Anastasiadis, S. H.; Floudas, G.; Fytas, G.; Pispas, S.; Hadjichristidis, N.; Pakula, T. *Macromolecules* **1996**, *29*, 1326.
(11) Leibler, L. *Macromolecules* **1980**, *13*, 1602.
(12) Fredrickson, G. H.; Helfand, E. *J. Chem. Phys.* **1987**, *87*, 697. See also Fredrickson, G. H.; Helfand, E.; Bates, F. S.; Leibler, L. In *Space-Time Organization in Macromolecular Fluids*; Tanaka, F., Doi, M., Ohta, T., Eds.; Springer-Verlag: Berlin, 1989.
(13) Matsen, M. W.; Bates, F. S. *Macromolecules* **1996**, *29*, 1091.
(14) Bates, F. S. *Science* **1991**, *251*, 898.
(15) Bartels, V. T.; Stamm, M.; Abetz, V.; Mortensen, K. *Europhys. Lett.* **1995**, *31*, 81.
(16) Owens, J. N.; Gancarz, I. S.; Koberstein, J. T.; Russell, T. P.; *Macromolecules* **1989**, *22*, 3380.
(17) Bates, F. S.; Rosedale, J. H.; Fredrickson, G. H. *J. Chem. Phys.* **1990**, *92*, 6255.
(18) Wolff, T.; Burger, C.; Ruland, W. *Macromolecules* **1993**, *26*, 1707.
(19) Winey, K. I.; Gobran, D. A.; Xu, Z. D.; Fetters, L. J.; Thomas, E. L. *Macromolecules* **1994**, *27*, 2392.
(20) Perahia, D.; Vacca, G.; Patel, S. S.; Dai, H. J.; Balsara, N. P. *Macromolecules* **1994**, *27*, 7645 and references therein.
(21) Floudas, G.; Pakula, T.; Fischer, E. W.; Hadjichristidis, N.; Pispas, S. *Acta Polym.* **1994**, *45*, 176.
(22) Sakamoto, N.; Hashimoto, T. *Macromolecules* **1995**, *28*, 6825. Ogawa, T.; Sakamoto, N.; Hashimoto, T.; Han, C. D.; Baek, D. M. *Macromolecules* **1996**, *29*, 2113.
(23) Sakamoto, N.; Hashimoto, T.; Han, C. D.; Kim, D.; Vaidya, N. Y. *Macromolecules* **1997**, *30*, 1621.
(24) Amundson, K.; Helfand, E.; Patel, S. S.; Quan, X.; Smith, S. D. *Macromolecules* **1992**, *25*, 1935.
(25) Rosedale, J. H.; Bates, F. S. *Macromolecules* **1990**, *23*, 2329.
(26) Han, C. D.; Baek, D. M.; Kim, J. K.; *Macromolecules* **1995**, *28*, 5886. Baek, D. M.; Han, C. D. *Polymer* **1995**, *36*, 4833.
(27) Hajduk, D. A.; Urayama, P.; Gruner, S. M.; Erramilli, S.; Register, R. A.; Brister, K.; Fetters, L. J. *Macromolecules* **1995**, *28*, 7148. Hajduk, D. A.; Gruner, S. M.; Erramilli, S.; Register, R. A.; Fetters, L. J. *Macromolecules* **1996**, *29*, 1473.
(28) Ashraf, A.; Smith, S. D.; Satkowski, M. M.; Spontak, R. J.; Clarson, S. J.; Lipscomb, G. G. *Polym. Prepr.* (*Am. Chem. Soc., Div. Polym. Chem.*) **1994**, *35*, 581. Smith, S. D.; Ashraf,

A.; Satkowski, M. M.; Spontak, R. J. *Polym. Prepr.* (*Am. Chem. Soc., Div. Polym. Chem.*) **1994**, *35*, 651. See also: Laurer, J. H.; Ashraf, A.; Smith, S. D.; Spontak, R. J. *Langmuir* **1997**, *13*, 2250.
(29) Hong, K. M.; Noolandi, J. *Macromolecules* **1983**, *16*, 1083. Whitmore, M. D.; Noolandi, J. *J. Chem. Phys.* **1990**, *93*, 2946.
(30) Hashimoto, T. In *Thermoplastic Elastomers: A Comprehensive Review*; Legge, N. R., Holden, G. Schroeder, H. E., Eds.; Hanser: Munich, 1987, and references therein.
(31) Connell, J. G.; Richards, R. W. *Macromolecules* **1990**, *23*, 1766.
(32) Balsara, N. P.; Perahia, D.; Safinya, C. R.; Tirrell, M.; Lodge, T. P. *Macromolecules* **1992**, *25*, 3896.
(33) Jian, T.; Anastasiadis, S. H.; Semenov, A. N.; Fytas, G.; Adachi, K.; Kotaka, T. *Macromolecules* **1994**, *27*, 4762.
(34) Lodge, T. P.; Pan, C.; Jin, X.; Liu, Z.; Zhao, J.; Maurer, W. W.; Bates, F. S. *J. Polym. Sci. B: Polym. Phys.* **1995**, *33*, 2289 and references therein.
(35) Olvera de la Cruz, M. *J. Chem. Phys.* **1989**, *90*, 1995.
(36) Fredrickson, G. H.; Leibler, L. *Macromolecules* **1989**, *22*, 1238.
(37) Hong, S.-U.; Stölken, S.; Zielinski, J. M.; Smith, S. D.; Duda, J. L.; Spontak, R. J. *Macromolecules* **1998**, *31*, 937.
(38) Caneba, G. T.; Soong, D. S.; Prausnitz, J. M. *J. Macromol. Sci.—Phys.* **1983**−**1984**, *B22*, 693.
(39) Krause, S.; Lu, Z.-H.; Iskandar, M. *Macromolecules* **1982**, *15*, 1076. Granger, A. T.; Krause, S.; Fetters, L. J. *Macromolecules* **1987**, *20*, 1421.
(40) Duda, J. L.; Kimmerly, G. K.; Sigelko, W. L.; Vrentas, J. S. *Ind. Eng. Chem. Fundam.* **1973**, *12*, 133..
(41) Widmaier, J. M.; Meyer, G. C. *J. Polym. Sci., Polym. Phys. Ed.* **1980**, *18*, 2217. See also: Hadziioannou, G.; Skoulios, A. *Macromolecules* **1982**, *15*, 258.
(42) Kane, L.; Satkowski, M. M.; Smith, S. D.; Spontak, R. J. *Macromolecules* **1996**, *29*, 8862; *J. Polym. Sci., B: Polym. Phys.* **1997**, *35*, 2653.
(43) Matsen, M. W.; Bates, F. S. *Macromolecules* **1995**, *28*, 7298.
(44) Hashimoto, T.; Yamasaki, K.; Koizumi, S.; Hasegawa, H. *Macromolecules* **1993**, *26*, 2895. Hashimoto, T.; Koizumi, S.; Hasegawa, H. *Macromolecules* **1994**, *27*, 1562.
(45) Spontak, R. J. *Macromolecules* **1994**, *27*, 6363.
(46) Matsen, M. W. *J. Chem. Phys.* **1995**, *103*, 3268.
(47) Mayes, A. M.; Russell, T. P.; Deline, V. R.; Satija, S. K.; Majkrzak, C. F. *Macromolecules* **1994**, *27*, 7447.
(48) Crank, J. *The Mathematics of Diffusion*; Oxford University Press: London, 1956.
(49) Overbergh, N.; Berghmans, H.; Smets, G. *Polymer* **1975**, *16*, 703.
(50) Vrentas, J. S.; Duda, J. L.; Hou, A.-C. *J. Appl. Polym. Sci.* **1984**, *29*, 399.
(51) Enscore, D. J.; Hopfenberg, H. B.; Stannett, V. T. *Polym. Eng. Sci.* **1980**, *20*, 1. See also Doghieri, F.; Sarti, G. C. *J. Polym. Sci., B: Polym. Phys.* **1997**, *35*, 2245.
(52) Vargaftik, N. B. *Handbook of Physical Properties of Liquids and Gases: Pure Substances and Mixtures*, 2nd ed.; Hemisphere: New York, 1975.
(53) Wood, L. A.; Rudd, J. F. In *Polymer Handbook*, 3rd ed.; Brandrup, J., Immergut, E. H., Eds.; Wiley-Interscience: New York, 1989.
(54) Vrentas, J. S.; Duda, J. L.; Ni, Y. C. *J. Polym. Sci., Polym. Phys. Ed.* **1977**, *15*, 2039.
(55) Duda, J. L.; Zielinski, J. M. In *Diffusion in Polymers*; Neogi, P., Ed.; Marcel Dekker: New York, 1996.

MA971516E